ACS APPLIED MATERIALS & INTERFACES

Research Article

www.acsami.org

Understanding the Role of Single Molecular ZnS Precursors in the Synthesis of In(Zn)P/ZnS Nanocrystals

Lifei Xi,[†] Deok-Yong Cho,[‡] Martial Duchamp,[§] Chris B. Boothroyd,[§] Jun Yan Lek,[∥] Astrid Besmehn,[⊥] Rainer Waser,[#] Yeng Ming Lam,*[,∥,#] and Beata Kardynal*[,†]

[†]Semiconductor Nanoelectronics (PGI-9), [§]Ernst Ruska-Centre and Peter Grünberg Institut, and [⊥]Central Institute for Engineering, Electronics and Analytics (ZEA-3), Forschungszentrum Jülich, 52425 Jülich, Germany

[‡]Department of Physics, Chonbuk National University, Jeonju 561-756, Republic of Korea

[∥]School of Materials Science and Engineering, Nanyang Technological University, 639798, Singapore

[#]Institute of Materials in Electrical Engineering and Information Technology 2 (IWE2), JARA-FIT, RWTH, Aachen D-52056, Germany

Supporting Information

ABSTRACT: Environmentally friendly nanocrystals (NCs) such as InP are in demand for various applications, such as biomedical labeling, solar cells, sensors, and light-emitting diodes (LEDs). To fulfill their potential applications, the synthesis of such high-quality "green" InP NCs required further improvement so as to achieve better stability, higher brightness NCs, and also to have a more robust synthesis route. The present study addresses our efforts on the synthesis of high-quality In(Zn)P/ZnS core−shell NCs using an air- and moisture-stable ZnS single molecular precursor (SMP) and In(Zn)P cores. The SMP method has recently emerged as a promising route for the surface overcoating of NCs due to its simplicity, high reproducibility, low reaction temperature, and flexibility in controlling the reaction. The synthesis involved heating the In(Zn)P core solution and $Zn(S_2CNR_2)$ (where R = methyl, ethyl, butyl, or benzyl and referred to as ZDMT, ZDET, ZDBT, or ZDBzT, respectively) in oleylamine (OLA) to 90−250 °C for 0.5−2.5 h. In this work, we systematically studied the influence of different SMP end groups, the complex formation and stability between the SMP and oleylamine (OLA), the reaction temperature, and the amount of SMP on the synthesis of high-quality In(Zn)P/ZnS NCs. We found that thiocarbamate end groups are an important factor contributing to the low-temperature growth of high-quality In(Zn)P/ZnS NCs, as the end groups affect the polarity of the molecules and result in a different steric arrangement. We found that use of SMP with bulky end groups (ZDBzT) results in nanocrystals with higher photoluminescence quantum yield (PL QY) and better dispersibility than those synthesized with SMPs with the shorter alkyl chain groups (ZDMT, ZDET, or ZDBT). At the optimal conditions, the PL QY of red emission In(Zn)P/ZnS NCs is 55 ± 4%, which is one of the highest values reported. On the basis of structural (XAS, XPS, XRD, TEM) and optical characterization, we propose a mechanism for the growth of a ZnS shell on an In(Zn)P core.

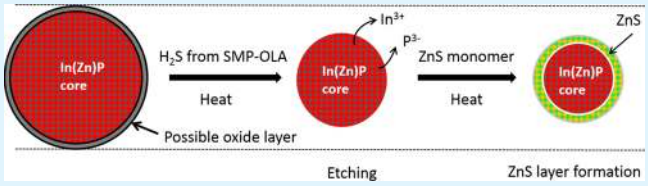

KEYWORDS: *core−shell, indium phosphide, zinc sulfide, single molecular precursor, complex, photoluminescence, quantum yield*

INTRODUCTION

The motivation for this study is to explore single molecular precursors (SMPs) for the synthesis of high-quality environmentally friendly In(Zn)P/ZnS nanocrystals (NCs) at low temperatures. Colloidal InP NCs have attracted a lot of interest because they have size-tunable photoluminescence (PL) emission wavelengths ranging from blue to the near-infrared (bulk band gap: 1.35 eV), larger exciton diameters, and low intrinsic toxicity compared with group II−VI compounds.[1−6] InP NCs can potentially be used for biomedical labeling, solar cells, sensors, and light-emitting diodes (LEDs).[2,3,7] However, compared to CdSe, as-prepared InP NCs exhibit rather poor optical properties due to nonradiative recombination at surface defects and surface traps.[7−9] Zinc sulfide (ZnS) is a nontoxic wide bandgap semiconductor material (bulk band gap: 3.61 eV), and one of the most important shell materials used for coating of a variety of group II−VI and group III−V semiconductor NCs.[10−12] The ZnS shell provides a physical barrier between the core and the surrounding medium, thus making the NCs less sensitive to environmental changes, surface chemistry, and photo-oxidation.[10] It also provides an efficient passivation of the dangling bonds of the cores and thus improves the PL intensity and luminescence decay time.[13,14]

A number of methods have been used to grow a ZnS shell on semiconductor NCs. These include the derived successive ionic layer adsorption and reaction (d-SILAR) method,[15−18] the one-pot heating-up procedure,[3] and thermal decomposition of the ZnS precursor mixture[19] and SMP.[20] The d-SILAR method was

Received: August 7, 2014
Accepted: September 24, 2014
Published: September 24, 2014

first reported for the deposition of Cu_2O thin films on glass substrates.[16] The films were formed by depositing one monolayer at a time by dipping the substrates alternately into a solution of Cu ions and a NaOH solution. The method is widely used for the deposition of thin films of binary and ternary metal chalcogenides or thin layers of oxides.[16,17] Li et al. used this method for the first time to grow high-quality CdSe/CdS core−shell NCs.[15] They alternatively injected Cd and S precursors into a solution containing CdSe NCs for the growth of a CdS shell. As d-SILAR is a step-by-step process, it provides relatively good control of the deposition process and of the shell thickness.[15,18] In the one-pot heating-up procedure all precursors are mixed at room temperature and subsequently heated to a reaction temperature (250−300 °C) at a very fast rate.[3] Li et al. pioneered the synthesis of highly luminescent InP/ZnS NCs using this method. Because of the difference in reactivity of the core and shell precursors, the InP cores form initially, followed by the growth of an overlayer of ZnS shell, leading to the formation of InP/ZnS NCs. This method improves the reproducibility and the possibility of large-scale NCs production. The NCs obtained with this method exhibited a narrow emission range (480−590 nm) limited by the possible InP core size and larger NCs for red light emission are needed for solid-state lighting.[3] Thermal decomposition of the ZnS precursor mixture was initially reported by Hines et al. in 1996.[19] In their study, two highly toxic and dangerous reagents, namely, zinc diethyl and bis(trimethylsilyl)sulfide, were added slowly into the CdSe core solution at 300 °C. Later, Haubold et al. employed this synthesis for InP/ZnS NCs.[21] Injecting a mixture of two precursors at such a high temperature may lead, however, to the formation of isolated ZnS NCs instead of a ZnS shell. It is also difficult to balance the reactivity of the two precursors.

Recently another method, based on the use of SMPs, emerged as a promising route for the surface overcoating of semiconductor and oxide.[22,23] SMPs are organometallic compounds that contain both the anionic groups, for example, O, S, or Se, and metal elements in one precursor. The strength of the metal−sulfur and sulfur−carbon bonds is different, which results in different thermal decomposition temperatures of these two bonds.[25] Thermal decomposition of these SMPs will result in the formation of metal oxide, chalcogenide, or alloy NCs.[22−25] SMPs, such as zinc dithiocarbamates and zinc ethylxanthate, have been used to synthesize CdS/ZnS,[20,26] CdSe/ZnS,[22,23,11] CdSe/CdS/ZnS,[27] CdTe/CdSe/ZnS,[28] and $CuInS_2$/ZnS.[29] Shell growth using SMPs offers many advantages. First, it is an air- and moisture-stable method, but not suitable for the air-sensitive core NCs. Second, it is a very simple route. It is a one-step and one-pot reaction, which avoids the need for typical multiple injection approaches, for example, in the d-SILAR method.[11,26,27] Third, it may be used at a lower reaction temperature compared to d-SILAR.[27,30] Finally, it provides flexibility in controlling the reaction.

To benefit fully from above advantages, a detailed understanding of the reaction kinetics/route of these SMPs on the quality of the NCs is important. This includes the stability of the SMP−oleylamine (OLA) complex, which is formed between Zn in the SMP with the amine group in OLA,[30] the thermal decomposition route, the effect of different end groups, the effect of reaction temperature, and the effect of the amount of SMP. For example, different end groups have different polarity and size (steric effect), thus affecting the ease of complex formation between the SMP and the amine, the reactivity of the complex, the decomposition temperature, and thus optical properties of the synthesized NCs.

A few studies on the use of the SMP method for ZnS shell growth for InP/ZnS NCs have been reported[2,5,7] For example, Xu et al. synthesized InP/ZnS NCs using the SMP and InP cores at 230 °C.[2] They found that a one-step and one-pot reaction using the SMP precursor avoids the necessity of typical multiple injections of the d-SILAR method. The quality of the resulting InP/ZnS NCs was comparable to that of the frequently used CdSe-based ones. Joung et al. found that the slow addition of the air-stable SMP at elevated temperature (200 °C) allowed ZnS shell formation on the surface of InP particle, thereby enhancing PL quantum yield (QY).[5] Yang et al. used SMPs for the secondary ZnS shell growth at 230 °C after starting the ZnS shell growth using the d-SILAR method.[7] However, the effect of reaction temperature and the amount of SMP required to modify the reaction significantly was not studied.

Here, we report our studies undertaken to understand the ZnS shell formation on In(Zn)P cores using SMPs. During the InP core synthesis, zinc carboxylate was added as it was found to improve QY of PL although the reason for this improvement is not clear.[2,7,12] Zinc carboxylates were proposed to play a role of stabilizing the surface, tuning the size/color, forming the In(Zn)P alloy structure as well as improving the optical characteristic of the NCs.[2,7,12] The function of zinc compound is not clear at this time. We found that, with the addition of zinc undecylenate, PL QY of core increased from less than 0.01% to 6.5%, while PL QY of In(Zn)P/ZnS was four times higher when other conditions are kept constant. We proposed that zinc undecylenate acts as a sacrificial agent to prevent the oxidation of indium precursor during the core synthesis as the redox potential is more favorable for the reduction of In. On the basis of our knowledge, this is the first report of a systematic study of the use of SMPs for shell coating on In(Zn)P NCs. Following comprehensive structural and optical characterization of such NCs, we propose a mechanism for the growth of In(Zn)P/ZnS NCs. For the first time, we report a study of the electronic structures in In(Zn)P/ZnS NCs using X-ray absorption spectroscopy (XAS), and the results reveal a number of details that have not been discussed before. The present synthesis work should benefit the potential applications of colloidal InP NCs in biomedical labeling, solar cells, sensors, and light-emitting diodes (LEDs).

RESULTS AND DISCUSSION

Morphology and Phase Analysis. Time-evolution X-ray diffraction (XRD) patterns of the as-prepared In(Zn)P core, In(Zn)P/ZnS NCs, and ZnS NCs, all synthesized using zinc dibenzyldithiocarbamate (ZDBzT) are shown in Figure 1. The XRD pattern from the In(Zn)P core shows three dominant peaks corresponding to the (111), (220), and (311) reflections of the zinc blende InP structure.[4,6,31] XRD spectra of the NCs extracted at different times during the shell growth show that the peak positions can be accounted for by the as prepared In(Zn)P core or zinc blende ZnS. This is an indication that the change in the spectra is stepwise. After 120 min of the reaction, the three peaks match those of zinc blende ZnS NCs synthesized from ZDBzT in an OLA/1-octadecene (ODE) mixture at 90° (see Figure 1). PL measured on the same set of samples showed a blue shift with reaction time (see Supporting Information, Figure S1). The fast PL blue shift within the first 60 min of reaction (which is the time when clear evidence of

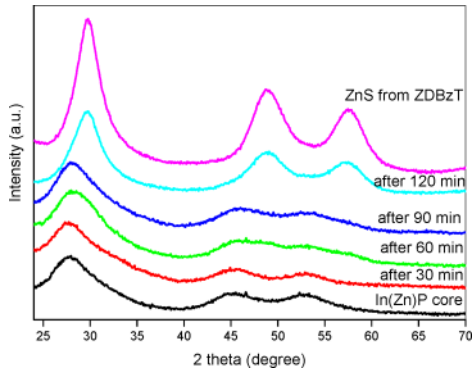

Figure 1. Time-evolution XRD patterns of the as-prepared In(Zn)P core, In(Zn)P/ZnS NCs synthesized from ZDBzT at 90 °C as a function of reaction time, and ZnS NCs synthesized from ZDBzT at 90 °C.

ZnS presence is first seen) indicates the size reduction of the In(Zn)P cores, which can be due to etching of the In(Zn)P core by H_2S gas generated from the decomposition of SMP–OLA complexes. Detailed discussion of the optical properties will be presented in the next section.

A high-resolution transmission electron microscopy (HRTEM) image of the In(Zn)P cores and In(Zn)P/ZnS NCs with ZnS shells synthesized using ZDBzT at 90 °C for 120 min are shown in Figure 2 (also refer to Supporting

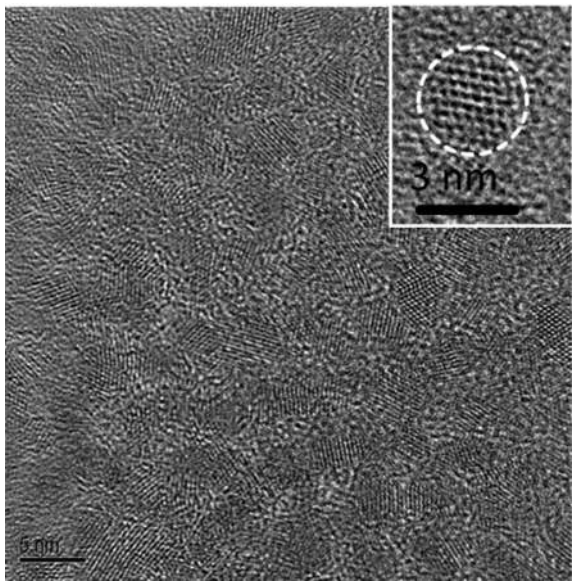

Figure 2. HRTEM image of In(Zn)P/ZnS NCs synthesized with ZDBzT after 120 min at 90 °C. (inset) Enlargement of an In(Zn)P core oriented along [110].

Information, Figure S2a for a TEM image of In(Zn)P core). The lattice fringes show that the In(Zn)P cores are single crystals, and the 0.34 ± 0.007 nm spacing is consistent with the (111) lattice plane spacing of zinc blend InP.[31] It can be seen that the good crystallinity of the NCs was maintained after the shell growth, while their size decreased from 3.15 ± 0.51 nm for the cores to 2.67 ± 0.46 nm for the core–shell NCs, in agreement with the blue shift in PL. The lattice fringe spacing was found to decrease to 0.33 ± 0.005 nm but remained bigger than that of bulk cubic ZnS (d = 0.31 nm). However, we found that there was a slight mismatch of the lattice constant between the calculated data and reported lattice constants. We found no match between our lattice constant and the values for other relevant compounds, such as cubic ZnS or wurtzite ZnS (see Supporting Information, Figure S2b). While a good match was found with α-Zn_3P_2, we verified that this compound cannot be synthesized under the conditions used (see Experimental Section). It has been reported that the synthesis of Zn_3P_2 requires very reactive zinc precursors, high temperature, and a long reaction time.[2,7] This implies that at the interface between InP and ZnS, due to the lattice mismatch between InP (a = 0.58687 nm) and ZnS (a = 0.54060 nm), the ZnS lattice is strained to adapt to the InP core lattice. This may inhibit a thick ZnS shell formation. Previous reports also mentioned that the surface chemical composition and crystal structure of InP NCs was modified during shell coating.[10,32,33]

To better understand what happened during shell growth, XAS spectra were collected from the samples. XAS probes empty electronic states and can be used for structural investigation of the materials.[34] In L_3-edge, S K-edge, and P K-edge XAS spectra from commercial bulk In_2O_3, In_2S_3, ZnS powders, and In(Zn)P/ZnS NCs synthesized with different SMPs or using the d-SILAR method are shown in Figure 3 (see also Supporting Information, Figure S3 for an XRD pattern and absorption and PL spectra of the same samples). Figure 3a shows that the In L_3-edge XAS spectra from In(Zn)P/ZnS NCs synthesized with the SMP method are identical for all of the precursors used. They are, however, different from the spectra of NCs synthesized with d-SILAR, bulk In_2S_3, and In_2O_3 powders, which are also different from each other. The difference between the spectra is even more visible in the derivatives shown in Figure 3b. The oxidation states of In ions in In_2S_3 and In_2O_3 are identical to each other as seen from the first maxima in the derivative spectra near 3731.2 eV. The oxidation states of all In(Zn)P/ZnS NCs are identical but slightly higher than those of In_2S_3 or In_2O_3 due to the different local structure (coordination). The XAS spectrum of the In(Zn)P/ZnS NCs synthesized with ZDBzT for 2 h still shows the same features (see Supporting Information, Figure S4a), indicating that the In(Zn)P cores are still preserved. There is an additional peak at 3733.8 eV in the spectra from NCs synthesized with SMPs, but this peak is absent from that prepared using d-SILAR. Since a similar In(Zn)P core is used, the presence of this peak in NCs from the SMP method implies that In L_3-edge originates from a more oxidized In species after the SMP shell formation reaction compared to the In(Zn)P core and In(Zn)P/ZnS NCs synthesized from the d-SILAR method. This new peak cannot be attributed to the band gap changes due to the incorporation of Zn because such a big energy shift (>1.5 eV) in XAS spectra was not observed in the X-ray photoelectron spectroscopy (XPS) spectra (see Supporting Information, Figure S5). To determine the origin of this peak we performed calculations of absorption energies with Zn incorporated into the InP lattice using the *ab initio* multiple scattering code, FEFF8.[35] The absorption energies of the lowest-energy peak were found to be at a higher oxidation state when In is surrounded by Zn rather than its own ions (see Supporting Information, Figure S4b). This peak could be the result of the incorporation of Zn atoms into the In(Zn)P core during shell coating. The absence of this peak in NCs from the d-SILAR method implies that shell growth occurs via a different route in both cases. This new feature cannot be assigned to In_2O_3 or In_2S_3 since neither the In_2O_3 nor the In_2S_3 reference spectra show such a feature (Figure 3b).

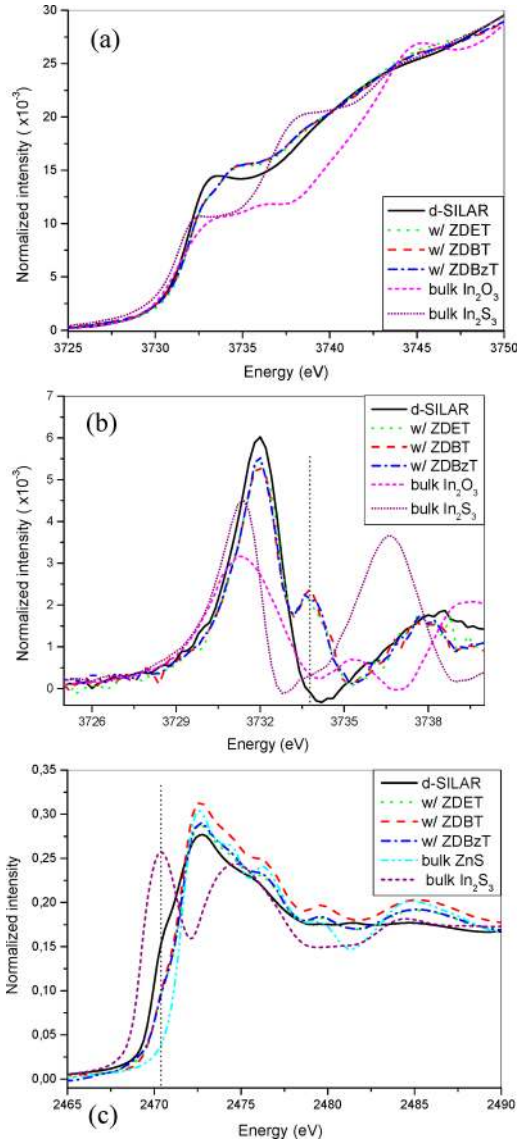

Figure 3. (a) In L_3-edge XAS, (b) In L_3-edge XAS derivatives and (c) S K-edge XAS spectra from In(Zn)P/ZnS NCs synthesized using SMPs or using the d-SILAR method. Spectra from commercial bulk In_2O_3, In_2S_3 and ZnS powders are also shown for comparison. The dash lines in (b) and (c) indicate an additional peaks at 3733.8 eV and a significant intensity increase at 2470.6 eV compared to ZnS powder, respectively.

Figure 3c shows the S K-edge XAS spectra from commercial In_2S_3, ZnS powder and In(Zn)P/ZnS NCs as synthesized with SMPs or the d-SILAR method. It can be seen that NCs have similar spectra to those of bulk ZnS, which very likely constitutes the shell around In(Zn)P cores. Interestingly, a significant increase in intensity near 2470.6 eV is observed for all NCs compared to bulk ZnS powder. This change is consistent with the incorporation of S into the surface of the In(Zn)P core to form In−S or S_x−In−P_{1-x} bond states.[32] Compared with In(Zn)P/ZnS NCs synthesized with the d-SILAR method, In(Zn)P/ZnS NCs synthesized with the SMP method have weaker features near 2470 eV, suggesting that there is a reduced formation probability of In−S or S_x−In−P_{1-x} bond states on the surface of the In(Zn)P core due to the lower synthesis temperature (90 °C) compared to the d-SILAR method (170 °C). This finding is consistent with previous studies, which showed that the d-SILAR method most likely produces a radially graded InPZnS alloy structure with a thin ZnS shell.[36] In this study, the In(Zn)P/ZnS NCs synthesized with the d-SILAR method showed lower optical quality in comparison to the corresponding SMP method. This observation is consistent with one previous study.[26] Thus, unless otherwise indicated, all In(Zn)P/ZnS NCs discussed subsequently are those synthesized using the SMP method.

Virieux et al. previously reported that a crystalline InP NC is surrounded by amorphous mixed oxides based on NMR and XPS studies.[4] They attributed this to the presence of carboxylate precursors in the solution. In this study, we used similar chemicals and synthesis methods for the In(Zn)P core but during the shell coating, the oxide layer is etched away from the surface of the In(Zn)P core as evident by the decreasing size of the NCs. The etching of the amorphous oxide layer from the surface of the In(Zn)P cores could also explain the change of P XPS signal (Figure 4a,b). The P 2p XPS spectrum from

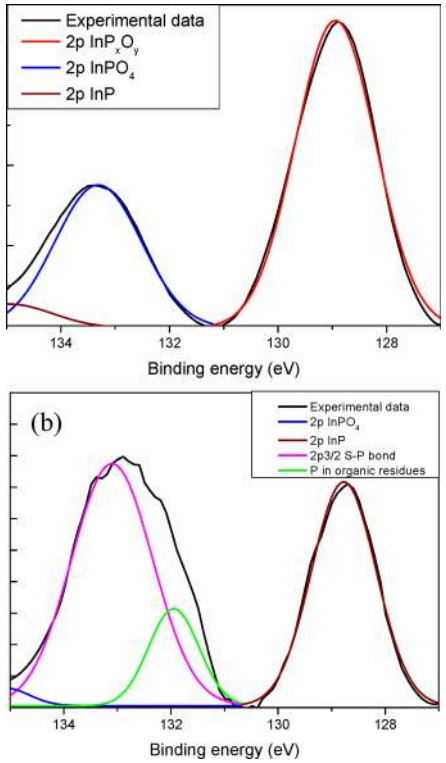

Figure 4. Fitted P 2p XPS spectra from (a) In(Zn)P core and (b) In(Zn)P/ZnS NCs.

In(Zn)P core shows two peaks: one characteristic of InP at 128.9 eV and one, with the dominant contribution at 133.3 eV, that can be assigned to indium phosphate oxide (InP_xO_y).[4,37] Following shell growth for 120 min, the intensity of InP at 128.8 eV decreased slightly and is shifted by 0.15 eV. The peak at ∼133 eV undergoes not only a larger shift but also a change in shape. The best fit to this peak is given by a sum of two peaks; one at 131.9 eV of unknown origin (probably organic residues containing P) and one at 133.0 eV, which has been observed on surfaces of InP treated with H_2S and has been interpreted as P−S bond.[38] This assignment should, however, be confirmed with NMR.[4] The XPS spectra contained signal from In, Zn, and S (see Supporting Information, Figure S5a−d), confirming the growth of the shell (the S peaks are in a

position characteristic of ZnS) and the presence of the core even after 2 h of shell coating. For example, a slight binding energy shift of the In 3d 5/2 XPS lines from 444.4 to 445.0 eV after 2 h is consistent with In being more positively ionized during shell coating, which is in good agreement with XAS studies. The Zn 2p 3/2 XPS line shifts from 1022.4 of the In(Zn)P core to 1021.8 eV of the In(Zn)P/ZnS NCs during the shell coating. The S 2p 3/2 XPS lines from In(Zn)P/ZnS NCs made with different reaction times shift slightly from 161.6 to 162.1 eV. This can be due to S incorporation into the In(Zn)P core, which is consistent with the S K-edge XAS results.[32,39]

Shell Growth. *1. Effect of the Different SMPs on the ZnS Coating.* In this study, four different SMPs were used for the ZnS shell. Figure 5 shows the chemical structures of the SMPs

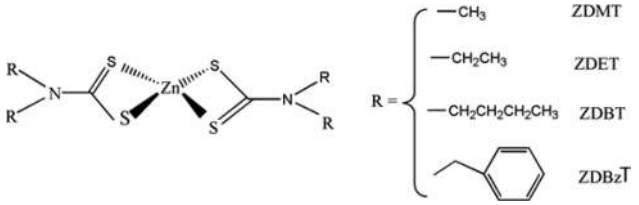

Figure 5. Chemical structures of the SMPs used in this study.

used in this study. This choice is to allow us to study the changes in the reactions leading to shell growth with the size and electron-donating capabilities of the end groups, which vary in increasing order: methyl < ethyl < butyl < benzyl. The latter is known to affect the electron density of the thiocarbonyl carbon ($R_2N-CS_2^-$) group in the SMP, thus affecting the C–S bond cleavage.[30,42] We investigated the effect of the different SMP end groups on the optical properties of the In(Zn)P/ZnS NCs. It was found that SMP with bulky end groups (ZDBzT) is better in terms of PL QY of NCs, reaction rate, and stability of the dispersion compared to those with small end groups such as zinc dimethyldithiocarbamate (ZDMT), zinc diethyldithiocarbamate (ZDET), or (zinc dibutyldithiocarbamate (ZDBT)). PL and UV–vis spectra from In(Zn)P/ZnS NCs synthesized with different SMPs are shown in Figure 6. It can be seen that both the PL emission and the UV–vis absorption spectra from In(Zn)P/ZnS NCs show a blue shift during the shell coating. In this study, we found that when other reaction conditions are kept constant, both ZDMT and ZDET produce In(Zn)P/ZnS NCs with 18–25 nm of blue emission shift with the PL QY ranging from 16 ± 3 to 25 ± 2% (see Figure 6a (inset)). Both ZDBT and ZDBzT produce In(Zn)P/ZnS NCs with a 20–38 nm blue emission shift and a PL QY ranging from 30 ± 3 to 38 ± 2%. The PL QY of In(Zn)P/ZnS NCs synthesized with ZDBzT is 6.5 times higher than that of In(Zn)P core. The full widths at half-maximum (fwhm) of the emission peaks are similar (~110 nm). A blue shift after shell coating has occasionally been reported for InP/ZnS NCs.[7,8] In the study by Ryu et al., zinc acetate was added to the InP core solution and heated up to 230 °C for 1–2 h prior to the addition of 1-dodecanethiol for ZnS shell growth.[8] The authors attributed the PL blue shift (9–22 nm) to surface etching by acetic acid, which is the reaction product of zinc acetate and palmitic acid. Recently, Lim et al. also proposed that the etching of small InP cores by residual acetic acid at moderate temperature (<150 °C) is the reason for the blue shift.[40] The residue acid as the origin of the blue shift in our case was ruled out in a control experiment in which the In(Zn)P core was heated and stirred in

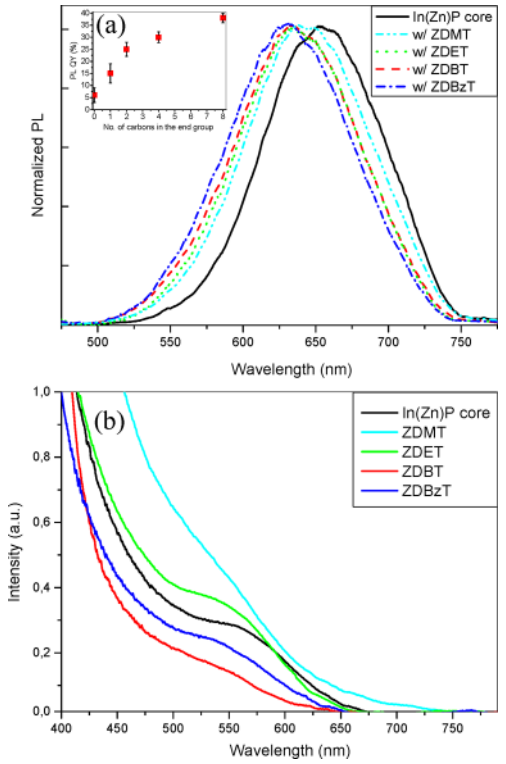

Figure 6. (a) PL and (b) UV–vis spectra from In(Zn)P/ZnS NCs synthesized with different SMPs at 90 °C after 120 min reaction. (inset) PL QY vs the number of carbons in the end groups of SMPs.

an OLA/ODE mixture overnight at 90 °C (which is the reaction temperature for comparing SMPs). PL of such treated NCs showed no blue shift. The rate at which the solution turns from dark red-brown through red and light red to orange during the shell formation is different for different precursors. ZDMT and ZDET solutions turned lighter at much slower rates compared to ZDBT and ZDBzT solutions. This is evident from the blue shift in the PL emission from the NCs obtained using ZDBT and ZDBzT solutions for the same reaction time (see Figure 6). In addition, the dispersibility of In(Zn)P/ZnS NCs synthesized with the shorter chains, for example, ZDMT or ZDET, is poorer in nonpolar solvents than that of the longer chain (ZDBT) or bulky (ZDBzT). The dispersibility of NCs is generally related to the type of surface capping ligand on the NCs.[41] This difference in solubility is an indication that the surface capping ligands were changed during shell coating.

Thermogravimetric analysis (TGA) can be used to determine changes in the sample composition during heating, the thermal stability of the sample, and kinetic parameters for chemical reactions. The results of TGA measurements from the four SMPs that decomposed under nitrogen are shown in Figure 7a (also refer to Supporting Information, Table S1). These SMPs decompose at a relatively high temperature and follow a single-stage process by gradually cleaving the $S-CNR_2$ bond.[42,43] With larger end groups, the decomposition temperature generally increases. It is because the end groups of the SMPs used differ not only in size but also in their electron-donating capabilities, thus affecting the C–S bond cleavage.[30,42,43] As shown using derivative thermogravimetry (DTG), which is useful in resolving reactions that occur at similar temperatures (Figure 7b), there is only one sharp peak in the curves, in good agreement with a single step-decomposition of the SMPs. The

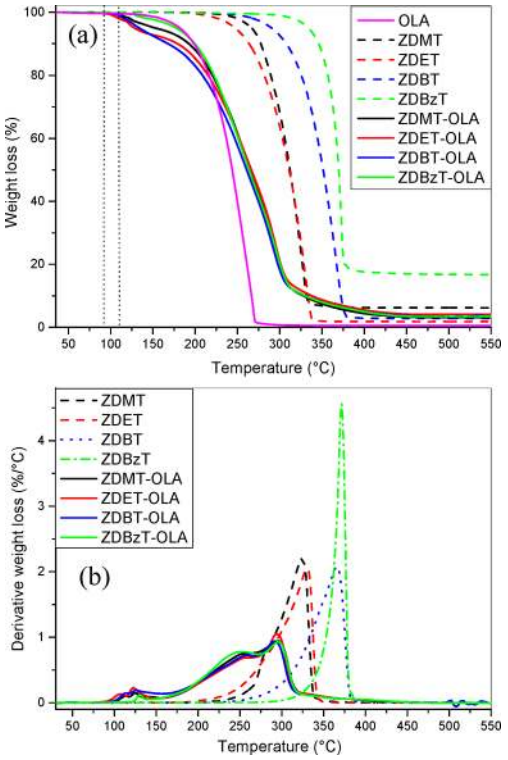

Figure 7. (a) TGA and (b) DTG curves from SMPs decomposed under nitrogen with and without OLA.

inflection temperatures (T_f) increase with the size of the end groups in the order ZDMT < ZDET < ZDBT < ZDBzT (also see Supporting Information, Table S2).

Figure 7a,b also shows data from SMPs with OLA decomposed under nitrogen. In this study, we added 0.152 mmol of pure SMP powder to 0.25 mL of OLA. The transformation to a clear solution is an indication of the formation of the SMP−OLA complex. With constant stirring at room temperature in an argon environment, the rate at which the solutions turn clear is quite different and follows the order: ZDMT < ZDET < ZDBT ≤ ZDBzT. This is consistent with the electron-donating capability of these four end groups. The end groups affect the electron density of thiocarbonyl carbon ($R_2N-CS_2^-$) in the SMP and thus the nucleophilic attack of the lone-pair electrons of nitrogen from OLA during complex formation.[30] In addition, the end groups can also affect the structure of the intermediate products of the reaction between OLA and the most electron-deficient thiocarbonyl carbon atoms of the SMPs and the subsequent condensation process that forms ZnS monomers by the C−S bond cleavage process.[30,42]

Figure 7 and Supporting Information, Table S1 show that the formation of the complex makes the SMP−OLA complex decompose at a much lower temperature than pure SMPs in agreement with previous studies.[26,30,42] The temperature at which decomposition starts for the four SMP−OLA complexes occurs in the range of 83−110 °C. This is in good agreement with previous reports that the reaction starting temperature for SMP−OLA could be as low as 80 °C.[11,26,30] Unlike for pure SMPs, DTG curves of complexes show a few overlapping peaks and shoulders, suggesting simultaneous reactions occur. In the early stages of the decomposition, there is a small peak around 110 °C for ZDMT, ZDET, and ZDBT but not for ZDBzT (see Supporting Information, Table S2). This is attributed to the fast release of H_2S gas. It is reported that H_2S gas can be detected at temperature as low as 80 °C for the SMP−OLA complex.[26] In control experiments, H_2S gas was also detected using a Ag^+ aqueous solution (see Experimental Section). A fast release of H_2S gas leads to a shorter period of etching and thus a smaller PL blue shift as shown in Figure 6a. There are three more features in the data from SMP−OLA decomposition, and they mark the evolution of other volatile products such as the secondary amine HNR_2 (R = methyl, ethyl, butyl, or benzyl) and alkylthiourea. The last two peaks may be related to cracking of the OLA and the thiourea hydrocarbon backbone. In Figure 7 and Supporting Information, Table S1, there are some variations in the residue from these SMPs. Only those from ZDBzT matched well with the calculated mass; the other values are lower than the calculated ones. Some possible reasons are the volatility of the nanoscale ZnS at higher temperatures and the volatility of some of the compounds formed during the reaction.[26]

FT-IR results from pure SMP and SMP−OLA complexes are shown in Table 1 and Supporting Information, Figure S6.

Table 1. FT-IR Measurements (cm^{-1}) from SMPs with and without OLA

compound	ν (N−H)	ν (C−N)	ν (C−S)
OLA	3319	1466	
ZDMT		1524	974
ZDET		1503	992
ZDBT		1495	956
ZDBzT		1481	982
ZDMT-OLA	3284	1490	980
ZDET-OLA	3286	1475	996
ZDBT-OLA	3235	1476	964
ZDBzT-OLA	3288	1464	975

There are many bands in the spectra of SMPs that are shifted after forming complexes with OLA. For example, an absorption band at 3235−3288 cm^{-1} in the spectra of these complexes is assigned to the ν(N−H) vibration of the complexed amine.[44] An additional absorption peak at ∼3219 cm^{-1} is assigned to the ν(N−H) stretching of the secondary amine (HNR_2).[44] The stretching frequency band at ∼1500 cm^{-1} due to polar >C═N^+ partial double bond stretching of $-S_2CNR_2$ moves to lower frequencies.[45] FT-IR spectra of In(Zn)P/ZnS NCs synthesized with different SMPs also suggest that a surface-capping ligand-exchange reaction happens during shell coating, and this affects the dispersibility of the NCs (see Supporting Information, Figure S6). After shell coating, the ═C−H aromatic stretching frequencies (3078, 3063, 3029) and the −C−H stretching frequency of the other three alkyl groups (methyl, ethyl, or butyl) are present in the FT-IR spectra of In(Zn)P/ZnS NCs. For example, the characteristic overtones for aromatics and C−C stretching from ZDBzT are seen from about 2000−1650 cm^{-1} and 1496 and 1465 cm^{-1} in In(Zn)P/ZnS NCs, which implies that benzylthiourea formed from the decomposition of SMP−OLA complex may be bound to the zinc atoms of the shell. The TGA results also showed a weight loss at the temperature range from 315 to 430 °C, which may be related to the decomposition of the small SMP molecules bound to NCs (see Supporting Information, Figure S7). It can be due to the decomposition of benzylthiourea on the In(Zn)P/ZnS NCs. However, quantitative information, such as the percentage of

replacement of carboxylate by benzylthiourea, is still missing, and further study is needed.

2. Influence of the Amount of SMP on the ZnS Coating. In this study, we used ZDBzT as the model SMP, and we found that with the total amount of reactant fixed, changing the amount of SMP changes the optical properties of the In(Zn)P/ZnS NCs substantially. First of all, the blue emission shift is larger with increasing amounts of SMP as shown in Figure 8a. It

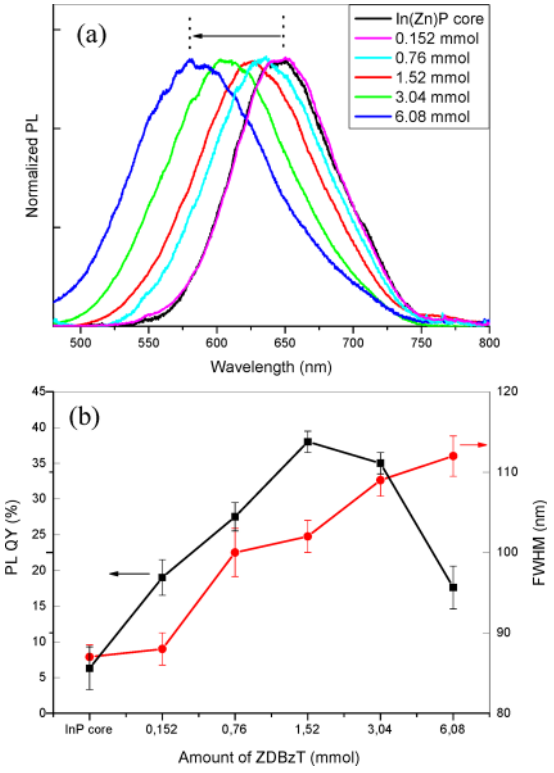

Figure 8. (a) Normalized PL spectra and (b) PL QY and fwhm from In(Zn)P/ZnS synthesized with varying amounts of ZDBzT and a 120 min reaction time.

is as large as 150 nm when the amount of SMP was increased by a factor of 4 with a 120 min reaction time compared with normal concentration (1.52 mmol of SMP per 7.0×10^{-7} mol of In(Zn)P cores). The rate at which the solution becomes brighter under UV light was also greatly accelerated. The color of the solution changed from dark red to orange-red within 60 min compared to 120 min for the normal concentration. This is consistent with the cores being etched and H_2S gas being evolved during shell formation. In addition, we found that when other conditions are kept constant, the sizes of core−shell NCs are smaller, and the PL emission becomes more blue-shifted when more SMP is used.

We found that the amount of SMP has a very strong effect on the quantum yield (QY) of the photoluminescence, and the optimum concentration of the SMP is 1.52 mmol per 7.0×10^{-7} mol of In(Zn)P cores, which results in a PL QY of 38 ± 2% at 90 °C. This value is 6 times higher than that of the In(Zn)P core. A further increase of the amount of SMP by a factor of 2 or 4 decreases the PL QY to 33 ± 1 or 17 ± 3%, respectively (see Figure 8b). Similarly, when the SMP amount was reduced to a half or a tenth, the reaction yields NCs with a PL QY of 28 ± 2 or 19 ± 3%, respectively. When a tenth amount was used, it was not sufficient for one monolayer of ZnS. The relatively high PL QY of NCs obtained implies that the shell coating is not a central issue. Other factors, for instance, surface oxides, can also affect the optical quality of NCs. The fwhm increases with the amount of SMPs. Quantitative XPS results of In(Zn)P core and In(Zn)P/ZnS NCs are shown in Supporting Information, Table S3. During the In(Zn)P core synthesis, Zn-to-In molar ratio of 0.50 was used, while XPS measurements showed Zn-to-In molar ratio of 0.32, which means that only a portion of zinc carboxylate was incorporated into the core. During the shell coating under the normal conditions (see Experimental Section), Zn-to-In and Zn-to-S molar ratios of 12.50 and 0.26 were used, while XPS measurements showed Zn to In and Zn to S molar ratios of 8.1 and 0.62, respectively. It implies an incomplete decomposition of SMP−OLA complex and possibly sulfur-rich surface NCs, for instance, thiourea bound to zinc atoms, which is consistent with the FT-IR results discussed above. We further calculated and found that the thickness of ZnS shell is 0.65 nm, corresponding to 2.1 monolayers. The yields of core synthesis and shell coating are 96 and 99%, respectively (refer to the Supporting Information).

3. Influence of the Reaction Temperature on the ZnS Coating. The reaction temperature for the model SMP (ZDBzT) was found to be another factor that affects the optical properties of NCs because cleavage of the C−S bond is a kinetic process.[42] The reaction was studied between 90 and 200 °C. It is found as the temperature is increased from 90 to 150, then to 170 °C, the PL QY of red emission NCs also increases from 38 ± 2, to 42 ± 1, then to 55 ± 4%. The PL QY of In(Zn)P/ZnS NCs synthesized with ZDBzT at 170 °C is 9 times higher than that of the In(Zn)P core. The enhanced PL QY is due to the faster and more complete SMP−OLA decomposition at the higher temperature. A further increase in temperature from 170 to 200 °C leads to a reduction of the PL QY to 41 ± 3% and an even larger blue shift. Previous work has shown that the dissolution of CdSe, CdSe/CdS, and CdSe/ZnS NCs was accelerated under elevated temperature and the presence of amine or acid.[46] Higher reaction temperature results in a smaller core−shell NCs when all the other conditions are kept constant. Thus, from this study, it was found that 170 °C and 1.52 mmol of ZDBzT are the optimum temperature and amount for high-quality In(Zn)P/ZnS NC synthesis, where a good balance between etching and ZnS shell growth can be achieved.

It is worth emphasizing that the PL QY of red emission In(Zn)P/ZnS NCs synthesized in this study is one of the highest values in the literature.[33,47] Kim et al. reported that the PL QY of red emission InP/GaP/ZnS NCs (λ = 615 nm) is ~58% after coating multishell for ZnInP cores.[33] Zan et al. synthesized InP/ZnS NCs with emission range of 540−660 nm, and the PL QY were ~30−60%.[47] Other studies showed much worse performance in terms of PL QY. In the work by Li et al., the PL QY of the NCs synthesized is less than 40% for emission higher than 600 nm, but at lower wavelength, their PL QY can be as high as 50−70%.[3] Xie et al. synthesized InP/ZnS NCs using d-SILAR method at 190 °C, canceling the pumping step, and achieved a PL QY of ~40%.[6] Yang et al. also found that the red emission InP/ZnS NCs showed less than 25% PL QY even after optimizing the molar ratio of InP to ZnS and using the d-SILAR and SMP methods for two-step shell coating.[7] Ryu et al. obtained 38% after optimizing the ratio of zinc acetate to phosphorus precursor.[8] A possible reason for this is the different shell coating methods used in these studies.

ZnS Shell Growth Mechanism. Scheme 1 shows the In(Zn)P/ZnS NCs formation using the SMP method deduced

Scheme 1. Schematic Illustration of the Formation of In(Zn)P/ZnS NCs from SMP Method

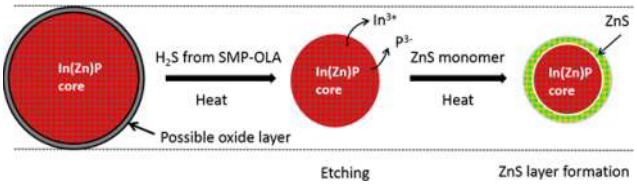

from the presented results. During the preheating and stirring (30 min) and the subsequent slow heating, the SMP−OLA complex is formed. When the temperature exceeds 83 °C, the SMP−OLA complex gradually decomposes and releases the H_2S gas, alkylthiourea, the secondary amine, and ZnS monomers in the solution.[30] At this stage the In(Zn)P cores are etched by the products of the thermal decomposition, mostly by H_2S gas. This results in a size reduction of the In(Zn)P cores as shown by TEM, UV−vis, and PL blue shifts. The InP surface oxide layer is also etched away. Oxygen atoms filling the vacancies on InP surface, predicted to act as deep traps, may also be etched away, and thus the PL QY is increased.[48] Further thermal decomposition of the SMP−OLA complex leads to a buildup of the concentration of ZnS monomers in the solution. When the concentration of ZnS monomers becomes high enough, the ZnS shell on the surface of the In(Zn)P cores starts forming as shown by the XRD data for t = 60 min. This slows down the etching with H_2S as seen from the reduced rate of the PL blue shift after some time (60 min of reaction as in Supporting Information, Figure S1). During the formation of the ZnS layer, the surface states of the In(Zn)P cores are gradually passivated; thus, the PL QY is improved. However, because the lattice mismatch between InP and ZnS is as large as 8%, the attachment of the ZnS layer to the In(Zn)P cores is not very favorable. The ZnS lattice is probably strained and adapts to the InP lattice, suggesting that only a thin layer of ZnS forms on the surface of the In(Zn)P core and mostly acts as a surface capping layer. Such a thin ZnS layer is nearly impossible to detect by HRTEM, energy dispersive spectroscopy (EDS), or electron energy loss spectroscopy (EELS). This explains why it is so difficult to obtain microscopic evidence in the presence of the ZnS shell on In(Zn)P cores.

In addition, the above proposed growth mechanism does not rule out the possibility of the existence of a complex shell structure due to ionic exchange.[29,32] Ionic exchange has been reported for the synthesis nanodots, nanorods, and nanowires in the solution as an alternative to conventional "hot-injection" method.[29,32,49] The ionic diffusion is thermodynamically favorable due to the thermodynamic instability of NCs and similar ionic radius.[4,29] However, ion exchange may be less likely due to two observations. XAS spectra shown in Figure 3c implied that there is very little presence of In−S in the NCs obtained using the SMP method compared to the d-SILAR method. On top of this, the XRD pattern evolution with time (refer to Figure 1) showed that the peaks existence can be accounted for by either In(Zn)P or ZnS, and there is no transition peak observed. If there is ion exchange, we would expect a gradual transition from one structure to the other.

CONCLUSION

In summary, we report a simple approach to the synthesis of high-quality In(Zn)P/ZnS core−shell NCs using air- and moisture-stable SMPs. The influence of different SMP end groups, the complex formation time, the amount of SMP, and the reaction temperature have been fully studied. We found that thiocarbamate end groups with a different polarity and steric effect have a decisive role in the quality of the low-temperature shell growth. They affect the complex formation between the SMP and the amine, the reactivity of the complex, the decomposition temperature, and the dispersibility of the NCs after shell coating. After a systematic comparison, optimal reaction conditions were proposed for In(Zn)P/ZnS NCs synthesis. Under these conditions, the PL QY of red emission In(Zn)P/ZnS NCs is 55 ± 4%, which is one of the highest values reported. It is also found that the PL QY of In(Zn)P/ZnS NCs synthesized with ZDBzT at 170 °C is 9 times higher than that of the In(Zn)P core. Finally, a mechanism for the growth of In(Zn)P/ZnS core−shell NCs based on XAS, XPS, XRD, TEM, and optical measurements has been proposed. An etching process due to the release of acidic gas (H_2S) from the decomposition of SMP−OLA complexes helps to remove any surface oxides from the surface of the In(Zn)P core during shell formation. During shell coating, the ZnS lattice is most likely strained to adapt to the InP lattice. A very thin ZnS layer forms on the surface of the In(Zn)P core and mostly acts as a surface-capping layer. These findings and the shell growth method should be useful for large-scale industrial production.

EXPERIMENTAL SECTION

Chemicals. Indium acetate (99.99%), stearic acid (SA, 95%), zinc undecylenate (99%), tris(trimethylsilyl)phosphine (PTMS, 98%), 1-dodecanethiol (DDT, 98%), Oleylamine (OLA, tech. 70%), chloroform (99.99%), and 1-octadecene (ODE, tech. 90%) were purchased from Sigma-Aldrich. Zinc dimethyldithiocarbamate (ZDMT, >95%), zinc diethyldithiocarbamate (ZDET, >99%), zinc dibutyldithiocarbamate (ZDBT, >97%), and zinc dibenzyldithiocarbamate (ZDBzT, >97%) were purchased from TCI Europe.

Synthesis of In(Zn)P Core NCs. Indium acetate (1 mmol), zinc undecylenate (0.5 mmol), SA (3.5 mmol), and ODE (20 mL) were mixed in a 25 mL flask. The Schlenk line was used for the synthesis, while glovebox was used for storage and preparation of a mixture of PTMS and ODE. The solution was heated to 100 °C and kept under a vacuum for 1 h. The solution was then purged with argon and heated to 300 °C. PTMS (1 mmol) in ODE (5 mL) was prepared inside a glovebox and rapidly injected to the flask. The reaction was carried out at 280 °C for 9 min. After that, the solution was quickly cooled to room temperature. Without any washing, the crude solution was stored in a fridge and used for shell growth. Different sized NCs can be obtained by adjusting the initial concentrations of In and phosphorus precursor, the type of carboxylate acid, the reaction temperature, and the reaction time. In this study, we focused on red-emission NCs.

Synthesis of In(Zn)P/ZnS NCs Using the SMP Method. The above crude solution (3.2 mL, which contains 7.0×10^{-7} mol of In(Zn)P NCs with a diameter of 3.15 nm, calculated as described earlier (refer to the Supporting Information for more details of the calculation)),[50] 10 mL of ODE, and 2.5 mL of OLA were mixed and stirred for 15 min. After that, 1.52 mmol of SMP was added. This is defined as the normal condition. The mixture was stirred for another 30 min. This time is sufficient for the formation of SMPs−OLA complex based on control experiments. The flask was evacuated and flushed with argon to obtain a water- and oxygen-free solution. The solution was then slowly heated to 90 °C over 30 min. After that, the temperature was held constant for another 2 h of reaction. During heating, the In(Zn)P core solution became brighter, which indicated a reaction of the SMP−OLA complex. After reaction, the solution was

allowed to cool to 50 °C. The NCs were precipitated from solution using acetone and centrifuged at 13 500 rpm for 15 min. The resulting NCs could be redispersed in chloroform, toluene, or other nonpolar solvents. To determine the effect of impurities from the In(Zn)P core solution, washed In(Zn)P cores were redispersed in ODE and used for shell growth using the SMP method. We found that the washing procedure did not help to improve the performance of the In(Zn)P/ZnS NCs. For other temperatures studied, we heated the solution containing the SMP and In(Zn)P cores directly to the temperature required.

Synthesis of In(Zn)P/ZnS NCs Using the d-SILAR Method. Zn stock solution: 0.2 mmol zinc undecylenate was mixed with 2 mL of ODE and heated to 130 °C to obtain a clear solution. DDT solution: 0.2 mmol of DDT was also mixed with 2 mL of ODE. 3.2 mL of the above crude solution and 10 mL of ODE were mixed for 15 min and heated to 170 °C. One milliliter of Zn stock solution was slowly injected. After 3 min, 1 mL of DDT solution was slowly injected. The above injection was repeated once with a 3 min interval. The reaction was stopped after 30 min. The same workup procedure was applied as described earlier.

Synthesis of ZnS NCs Using SMP. The reaction conditions were the same as above for shell growth using the SMP method. The only difference was the absence of the In(Zn)P core solution.

Synthesis of Zn_3P_2 NCs. The reaction conditions were the same as above for the In(Zn)P core growth using the hot injection method. The only difference was the absence of the indium acetate. We found that the color of the solution did not change after the injection of a mixture of PTMS and ODE even after 1 h of reaction.

Detection of H_2S Gas Using a Ag^+ Solution. During the synthesis of In(Zn)P/ZnS NCs using the SMP method, argon gas was passed into the reaction flask and then into an aqueous solution of $AgNO_3$. The clear and colorless $AgNO_3$ solution turned gray and then black within 2 h.

Characterization. Absorption spectra were measured using an ATI unicam UV 2−400 UV−vis spectrophotometer. Emission spectra were obtained using a homemade PL setup. The excitation wavelength (405 nm) is generated from a laser source. The laser beam is focused to a spot with an achromatic objective lens. PL from the investigated sample is collected and collimated with the same lens and is then transmitted through the dichroic mirror into the detection part of the system. A spectrometer (Andor 303i) was equipped with an Andor iDus Si CCD camera on output. The beam was focused on a 10 mm quartz cuvette. The acquisition was performed using the Andor software. The system was calibrated using a lamp with a known spectrum, which allows conversion of the counts recorded on the CCD into photons/nm/m^2. All the experiments were carried out at room temperature. The QYs of the In(Zn)P and In(Zn)P/ZnS NCs were measured by comparison with rhodamine 6G (Sigma, 83697, QY = 95%) and rhodamine 101 (Sigma, 83694, QY = 95%) in absolute ethanol.[51] The optical density (OD) at the excitation wavelength of the NCs and a dye sample was set at the same value. The ODs at the first exciton absorption peak of the NCs and the reference samples were less than 0.1 to reduce the error from reabsorption. Finally, the QY of the QD sample was obtained by comparing the integrated area of PL emission of the NCs and the reference samples.

TEM and HRTEM were taken on JEOL 2100F and FEI Titan "Pico" microscopes with an acceleration voltage of 200 kV. X-ray absorption spectroscopy (XAS) spectra from In(Zn)P/ZnS NCs synthesized with different SMPs, bulk In_2O_3, In_2S_3, and ZnS powders were collected on the 16A1 (Tender X-ray Absorption) beamline at the NSRRC in Taiwan. Data were collected in fluorescence yield mode with a Lytle detector (Lytle, 1999) at room temperature and analyzed with Athena. In L_3-edge, P K-edge, and S K-edge XAS spectra were collected from those samples. NCs were deposited on a Si wafer, while other reference powders were gently put on a Kapton tape with a brush. XPS was performed under ultrahigh vacuum using a PHI5000 VersaProbe II with monochromatic Al Kα radiation in a large area mode (1.4 mm × 200 μm, 100W, 20 kV). A 20 eV pass energy was used for the elemental scans. Quantification of the survey scans was accomplished using MULTIPAK software. Core-level spectra were fitted with a mixed Gauss-Lorentz function after subtraction of a Shireley-background. Fourier transform infrared (FT-IR) spectra were recorded on a Nexus 470 spectrometer (Thermo Nicolet) using the transmission mode. XRD patterns were recorded on an X'Pert PRO PANalytical system from Phillips with Cu Kα irradiation (λ = 0.154 06 nm). TGA was carried out using a TGA Q500 or 2950 apparatus under nitrogen flow with a heating rate of 10 °C/min.

■ ASSOCIATED CONTENT

Supporting Information

Additional tables, PL spectra, power spectrum of an HRTEM image, XRD patterns, XAS spectra, XPS surveys and elemental results, UV−vis spectra, FT-IR spectra, TGA curves, and calculations for shell growth (PDF). This material is available free of charge via the Internet at http://pubs.acs.org.

■ AUTHOR INFORMATION

Corresponding Authors

*E-mail: YMLam@ntu.edu.sg. (Y.M.L.)
*E-mail: B.Kardnal@fz-juelich.de. (B.K.)

Notes

The authors declare no competing financial interest.

■ ACKNOWLEDGMENTS

This work is supported by the NWs4LIGHT project. We thank Prof. Dr. A. Böker and Dr. W. Tillmann (Leibniz-Institut für Interaktive Materialien (DWI), RWTH Aachen University) for assistance with the FT-IR measurements. M.D. acknowledges financial support from the European Union under the Seventh Framework Programme under a contract for an Integrated Infrastructure Initiative (No. 312483-ESTEEM2). B.K. and Y.M.L. acknowledge the support from BMBF and NTU under the 1° N Programme.

■ REFERENCES

(1) Battaglia, D.; Peng, X. Formation of High Quality InP and InAs Nanocrystals in a Noncoordinating Solvent. *Nano Lett.* **2002**, *2*, 1027−1030.

(2) Xu, S.; Ziegler, J.; Nann, T. Rapid synthesis of highly luminescent InP and InP/ZnS nanocrystals. *J. Mater. Chem.* **2008**, *18*, 2653−2656.

(3) Li, L.; Reiss, P. One-Pot Synthesis of Highly Luminescent InP/ZnS Nanocrystals without Precursor Injection. *J. Am. Chem. Soc.* **2008**, *130*, 11588−11589.

(4) Virieux, H.; Le Troedec, M.; Cros-Cagneux, A.; Ojo, W.-S.; Delpech, F.; Nayral, C.; Martinez, H.; Chaudret, B. InP/ZnS Nanocrystals: Coupling NMR and XPS for Fine Surface and Interface Description. *J. Am. Chem. Soc.* **2012**, *134*, 19701−19708.

(5) Joung, S. M.; Yoon, S. C.; Han, S.; Kim, Y.; Jeong, S. Facile Synthesis of Uniform Large-sized InP Nanocrystal Quantum Dots Using Tris(tert-butyldimethylsilyl)phosphine. *Nanoscale Res. Lett.* **2012**, *7*, 93.

(6) Xie, R. G.; Battaglia, D.; Peng, X. G. Colloidal InP Nanocrystals as Efficient Emitters Covering Blue to Near-infrared. *J. Am. Chem. Soc.* **2007**, *129*, 15432−15433.

(7) Yang, X.; Zhao, D.; Leck, K. S.; Tan, S. T.; Tang, Y. X.; Zhao, J.; Demir, H. V.; Sun, X. W. Full Visible Range Covering InP/ZnS Nanocrystals with High Photometric Performance and Their Application to White Quantum Dot Light-Emitting Diodes. *Adv. Mater.* **2012**, *24*, 4180−4185.

(8) Ryu, E.; Kim, S.; Jang, E.; Jun, S.; Jang, H.; Kim, B.; Kim, S. W. Step-Wise Synthesis of InP/ZnS Core−Shell Quantum Dots and the Role of Zinc Acetate. *Chem. Mater.* **2009**, *21*, 573−575.

(9) Reiss, P. In *Semiconductor Nanocrystal Quantum Dots: Synthesis, Assembly, Spectroscopy and Applications;* Rogach, A. L., Ed.; Springer: New York, 2008; Chapter 2, pp 35−72.

(10) Reiss, P.; Protiere, M.; Li, L. Core/Shell Semiconductor Nanocrystals. *Small* **2009**, *5*, 154−168.
(11) Dethlefsen, J. R.; Døssing, A. Preparation of a ZnS Shell on CdSe Quantum Dots Using a Single-Molecular Precursor. *Nano Lett.* **2011**, *11*, 1964−1969.
(12) Thuy, U. T. D.; Reiss, R.; Liem, N. Q. Luminescence Properties of In(Zn)P Alloy Core/ZnS Shell Quantum Dots. *Appl. Phys. Lett.* **2010**, *97*, 193104.
(13) Shirazi, R.; Kopylov, O.; Kovacs, A.; Kardynal, B. E. Temperature Dependent Recombination Dynamics in InP/ZnS Colloidal Nanocrystals. *Appl. Phys. Lett.* **2012**, *101*, 091910.
(14) Thuy, P. T.; Thuy, U. T. D.; Chi, T. T. K.; Phuong, L. Q.; Liem, N. Q.; Li, L.; Reiss, R. Comparative Photoluminescence Study of Close-packed and Colloidal InP/ZnS Quantum Dots. *J. Phys.: Conf. Ser.* **2009**, *187*, 012014.
(15) Li, J.; Wang, Y.; Guo, W.; Keay, J. C.; Mishima, T. D.; Johnson, M. B.; Peng, X. Large-Scale Synthesis of Nearly Monodisperse CdSe/CdS Core/Shell Nanocrystals Using Air-Stable Reagents via Successive Ion Layer Adsorption and Reaction. *J. Am. Chem. Soc.* **2003**, *125*, 12567−12575.
(16) Ristov, M.; Sinadinovski, G. J.; Grozdanov, I. Chemical deposition of Cu 2O thin films. *Thin Solid Films* **1985**, *123*, 63−67.
(17) Pathan, H. M.; Lokhande, C. D. Deposition of Metal Chalcogenide Thin Films by Successive Ionic Layer Adsorption and Reaction (SILAR) Method. *Bull. Mater. Sci.* **2004**, *27*, 85−111.
(18) Dubal, D. P.; Holze, R. A Successive Ionic Layer Adsorption and Reaction (SILAR) Method to Induce Mn_3O_4 Nanospots on CNTs for Supercapacitors. *New J. Chem.* **2013**, *37*, 403−408.
(19) Hines, M. A.; Guyot-Sionnest, P. Synthesis and Characterization of Strongly Luminescing ZnS-Capped CdSe Nanocrystals. *J. Phys. Chem.* **1996**, *100*, 468−471.
(20) Protiere, M.; Reiss, P. Facile Synthesis of Monodisperse ZnS Capped CdS Nanocrystals Exhibiting Efficient Blue Emission. *Nanoscale Res. Lett.* **2006**, *1*, 62−67.
(21) Haubold, S.; Haase, M.; Kornowski, A.; Weller, H. Strongly Luminescent InP/ZnS Core−Shell Nanoparticles. *ChemPhysChem* **2001**, *2*, 331.
(22) Malik, M. A.; O'Brien, P.; Revaprasadu, N. A Simple Route to the Synthesis of Core/Shell Nanoparticles of Chalcogenides. *Chem. Mater.* **2002**, *14*, 2004−2010.
(23) Revaprasadu, N.; Malik, M. A.; O'Brien, P.; Wakefield, G. A Simple Route to Synthesise Nanodimensional CdSe−CdS Core−Shell Structures from Single Molecule Precursors. *Chem. Commun.* **1999**, 1573−1574.
(24) Pan, D. C.; Weng, D.; Wang, X. L.; Xiao, Q. F.; Chen, W.; Xu, C. L.; Yang, Z.; Lu, Y. Alloyed semiconductor nanocrystals with broad tunable band gaps. *Chem. Commun.* **2009**, 4221−4223.
(25) Hogarth, G. In *Prog. Inorg. Chem.;* Karlin, K. D., Ed.; Wiley: Hoboken, NJ, 2005; Chapter 2, pp 1978−2003.
(26) Chen, D.; Zhao, F.; Qi, H.; Rutherford, M.; Peng, X. Bright and Stable Purple/Blue Emitting CdS/ZnS Core/Shell Nanocrystals Grown by Thermal Cycling Using a Single-Source Precursor. *Chem. Mater.* **2010**, *22*, 1437−1444.
(27) Chen, G. J.; Zhang, W. J.; Zhong, X. H. Single-source Precursor Route for Overcoating CdS and ZnS Shells Around CdSeCore Nanocrystals. *Front. Chem. China* **2010**, *5*, 214−220.
(28) Zhang, W. J.; Chen, G. J.; Wang, J.; Ye, B. C.; Zhong, X. H. Design and Synthesis of Highly Luminescent Near-infrared-emitting Water-soluble CdTe/CdSe/ZnS Core/shell/shell Quantum Dots. *Inorg. Chem.* **2009**, *48*, 9723−9731.
(29) Park, J.; Kim, S.-W. $CuInS_2$/ZnS Core/shell Quantum Dots by Cation Exchange and Their Blue-shifted Photoluminescence. *J. Mater. Chem.* **2011**, *21*, 3745−3750.
(30) Jung, Y. K.; Kim, J. I.; Lee, J.-K. Thermal Decomposition Mechanism of Single-Molecule Precursors Forming Metal Sulfide Nanoparticles. *J. Am. Chem. Soc.* **2010**, *132*, 178−184.
(31) Micic, O. I.; Curtis, C. J.; Jones, K. M.; Sprague, J. R.; Nozik, A. J. Synthesis and Characterization of InP Quantum Dots. *J. Phys. Chem.* **1994**, *98*, 4966−4969.
(32) Huang, K.; Demadrille, R.; Silly, M. G.; Sirotti, F.; Reiss, P.; Renault, O. Internal Structure of InP/ZnS Nanocrystals Unraveled by High-Resolution Soft X-ray Photoelectron Spectroscopy. *ACS Nano* **2010**, *4*, 4799−4805.
(33) Kim, S.; Kim, T.; Kang, M.; Kwak, S. K.; Yoo, T. W.; Park, L. S.; Yang, I.; Hwang, S.; Lee, J. E.; Kim, S. K.; Kim, S. W. Highly Luminescent InP/GaP/ZnS Nanocrystals and Their Application to White Light-Emitting Diodes. *J. Am. Chem. Soc.* **2012**, *134*, 3804−3809.
(34) Mino, L.; Agostini, G.; Borfecchia, E.; Gianolio, D.; Pivano, A.; Gallo, E.; Lamberti, C. Low-dimensional Systems Investigated by X-ray Absorption Spectroscopy: a Selection of 2D,1D and 0D Cases. *J. Phys. D: Appl. Phys.* **2013**, *46*, 423001.
(35) Ankudinov, A. L.; Ravel, B.; Rehr, J. J.; Conradson, S. D. Real-space Multiple-scattering Calculation and Interpretation of X-ray-Absorption Near-edge Structure. *Phys. Rev. B* **1998**, *58*, 7565.
(36) Li, L.; Protiere, M.; Reiss, P. Economic Synthesis of High Quality InP Nanocrystals Using Calcium Phosphide as the Phosphorus Precursor. *Chem. Mater.* **2008**, *20*, 2621−2623.
(37) Bouchikhi, B.; Michel, C.; Ravelet, S.; Lepley, B. Preparation and Electrical Properties of Thin Native Oxide Double-layer Insulator Films on n-type InP. *Phys. Status Solidi A* **1987**, *101*, 173−184.
(38) Nelson, A. J.; Frigo, S.; Rosenberg, R. Soft X-ray Photoemission Characterization of the H_2S Exposed Surface of p-InP. *J. Appl. Phys.* **1992**, *71*, 6086−6089.
(39) Huang, W. H.; Chen, H. C.; Chang, C. C.; Hsieh, J. T.; Hwang, H. L. Adsorption and Decomposition of H_2S on InP(100). *J. Phys. Chem. B* **1999**, *103*, 3663−3668.
(40) Lim, K.; Jang, H. S.; Woo, K. Synthesis of Blue Emitting InP/ZnS Quantum Dots through Control of Competition between Etching and Growth. *Nanotechnology* **2012**, *23*, 485609.
(41) Xi, L. F.; Lam, Y. M. Controlling Growth of CdSe Nanowires through Ligand Optimization. *Chem. Mater.* **2009**, *21*, 3710−3718.
(42) van Poppel, L. H.; Groy, T. L.; Caudle, M. T. Carbon−Sulfur Bond Cleavage in Bis(*N*-alkyldithiocarbamato)cadmium(II) Complexes: Heterolytic Desulfurization Coupled to Topochemical Proton Transfer. *Inorg. Chem.* **2004**, *43*, 3180−3188.
(43) Memon, A. A.; Afzaal, M.; Malik, M. A.; Nguyen, C. Q.; O'Brien, P.; Raftery, J. The N-alkyldithiocarbamato Complexes $[M(S_2CNHR)_2]$ (M = Cd(II) Zn(II); R = C_2H_5, C_4H_9, C_6H_{13}, $C_{12}H_{25}$); Their Synthesis, Thermal Decomposition and Use to Prepare of Nanoparticles and Nanorods of CdS. *Dalton Trans.* **2006**, 4499−4505.
(44) Higgins, G. M. C.; Saville, B. Complexes of Amines with Zinc Dialkyldithiocarbamates. *J. Chem. Soc.* **1963**, 2812−2817.
(45) Adli, H. K.; Sidek, N. M.; Ismail, N.; Khairul, W. M. Several Organotin (IV) Complexes Featuring 1-Methylpiperazinedithiocarbamate and N-Methylcyclohexyldithiocarbamate as Ligands and Their Anti-Microbial Activity Studies. *Chiang Mai J. Sci.* **2013**, *40*, 117−125.
(46) Siy, J. T.; Bartl, M. H. Insights into Reversible Dissolution of Colloidal CdSe Nanocrystal Quantum Dots. *Chem. Mater.* **2010**, *22*, 5973−5982.
(47) Zan, F.; Ren, J. Gas-liquid phase synthesis of highly luminescent InP/ZnS core/shell quantum dots using zinc phosphide as a new phosphorus source. *J. Mater. Chem.* **2012**, *22*, 1794−1799.
(48) Fu, H. X.; Zunger, A. InP Quantum Dots: Electronic Structure, Surface Effects, and the Redshifted Emission. *Phys. Rev. B* **1997**, *56*, 1496−1508.
(49) Xi, L. F.; Lek, J. Y.; Liang, Y. N.; Boothroyd, C.; Zhou, W.; Yan, Q.; Hu, X.; Chiang, F. B. Y.; Lam, Y. M. Stability studies of CdSe nanocrystals in an aqueous environment. *Nanotechnology* **2011**, *22*, 275706.
(50) Yu, W. W.; Qu, L. H.; Guo, W. Z.; Peng, X. G. Experimental Determination of the Extinction Coefficient of CdTe, CdSe, and CdS Nanocrystals. *Chem. Mater.* **2003**, *15*, 2854−2860.
(51) Grabolle, M.; Spieles, M.; Lesnyak, V.; Gaponik, N.; Eychmüller, A.; Resch-Genger, U. Determination of the Fluorescence Quantum Yield of Quantum Dots: Suitable Procedures and Achievable Uncertainties. *Anal. Chem.* **2009**, *81*, 6285−6294.